ASTM INTERNATIONAL

Materials Performance and Characterization

U. V. Nayak[1] and K. N. Prabhu[2]

DOI: 10.1520/MPC20180084

Effect of Section Thickness on Heat Transfer during Quenching in Vegetable Oils

VOL. 7 / NO. 1 / 2018

Materials Performance and Characterization

doi:10.1520/MPC20180084 / Vol. 7 / No. 1 / 2018 / available online at www.astm.org

U. V. Nayak[1] and K. N. Prabhu[2]

Effect of Section Thickness on Heat Transfer during Quenching in Vegetable Oils

Reference

Nayak, U. V. and Prabhu, K. N., "Effect of Section Thickness on Heat Transfer during Quenching in Vegetable Oils," *Materials Performance and Characterization*, Vol. 7, No. 1, 2018, pp. 384–396, https://doi.org/10.1520/MPC20180084. ISSN 2379-1365

ABSTRACT

In the present work, mineral, sunflower, karanja, and neem oil were used as quench media. 304 stainless steel probes with diameters of 25 mm and 50 mm were quenched in these oils to assess the effect of section diameter on heat transfer during quenching. Cooling curve analysis was carried out by instrumenting the probes at various locations with thermocouples. The heat extraction ability of oil quench media was quantified using an inverse heat conduction method. Thermal data and the predicted hardness values showed the suitability of nonedible vegetable oils as potential quenchants to heat treat steels. The predicted hardness was higher during quenching in karanja oil compared to other oil media.

Keywords

quenching, section thickness, vegetable oils, spatiotemporal heat flux

Manuscript received June 2, 2018; accepted for publication July 30, 2018; published online September 12, 2018.

[1] Department of Metallurgical and Materials Engineering, National Institute of Technology Karnataka, Srinivasnagar PO, Surathkal, Mangalore 575025, India

[2] Department of Metallurgical and Materials Engineering, National Institute of Technology Karnataka, Srinivasnagar PO, Surathkal, Mangalore 575025, India (Corresponding author), e-mail: prabhukn_2002@yahoo.co.in, https://orcid.org/0000-0002-8359-2587

Introduction

Oil quenchants are the most popularly used quenching media for hardening steels. They have been shown to produce satisfactory mechanical properties, with tolerable unwanted distortions [1] compared to water. Oil quench media are petroleum, or animal, or vegetable based. Of the oil quench media available, petroleum-based mineral oils occupy a dominating share and have been used for decades in the heat treatment industry to harden steels [2]. These oils derived from petroleum base stocks are refined, distilled, purified, and various additives are added to it to cater to specific applications. Based on the specific purpose of the utilization of mineral oil as quench media, they are classified as cold,

accelerating, and hot oils [3]. However, mineral oils pollute the environment because they are derived from nonrenewable sources. Smoke and fire hazards are other drawbacks that can increase the operational risks leading to significant losses of life and property [4]. These disadvantages can be countered using vegetable oils as quench media. Vegetable oils are derived from plant sources and are renewable. Their use is eco-friendly compared to the use of mineral oils. An unstable vapor phase stage was reported in the work of Rose concerning the use of rapeseed oil as quench medium [5]. Vegetable oils have high flash and fire temperature (typically above 280°C) compared to mineral oils (typically below 220°C). Vegetable oils have a higher boiling point because of the C==C in them, and their boiling point is well above those of mineral oils. Several vegetable oils were tested for their quench performance and compared with mineral oils by de Souza et al. [6]. The critical cooling parameters reported by them show that the cooling rate occurs at a temperature of 700°C, which is higher than that seen for mineral oils. Further, the time during which the vapor phase stage existed was lower for vegetable oils compared to mineral oils. It was also found that the vegetable oils had a higher viscosity and viscosity index compared to the mineral oils used. The higher viscosity index for vegetable oils signifies the stability in viscosity with increased temperature for the vegetable oils. The quenching ability of vegetable oils using inconel 600 alloy probe have been quantified by many researchers and their results showed that vegetable oils were better compared to mineral oils. However, most of the vegetable oils used as quench media were edible oils. Use of such oils for an industrial heat treatment purpose will cause a shortfall for processing food. A preferable alternative to this is to explore the possibility of nonedible vegetable oils as quenching media. A detailed study on the feasibility of nonedible pongamia pinnata was done by Ramesh and Prabhu [7]. Their results showed faster cooling and spreading of pongamia compared to mineral oil. Further, the rewetting front, which is defined as the loci of points separating the vapor phase stage from the nucleate boiling stage, was found to be more uniform than during quenching with mineral oil. Nonedible jetropa oil had higher severity compared to mineral oil Adekunle, Adebiyi, and Durowoju et al. [8]. Ademoh [9] showed the feasibility to austemper 0.16 carbon steel in neem oil.

In the present work, two nonedible vegetable oils, namely karanja and neem oil, were used as quench media. Their quench performance was analyzed and compared against that of sunflower oil and a mineral oil. Stainless steel (SS) probes with section diameters of 25 and 50 mm were quenched to obtain the quenching ability of oils with section thickness. In most of the literatures, cited inconel 600 alloy probes or other similar metal pieces that are of small sizes are used. The information obtained with such a study is useful only for the characterization of quench media. Small-sized inconel probes do not provide any information regarding the quenching ability of the oil for hardening steels of large sizes. The heat flux transients at the metal/quenchant interface was estimated using the inverse heat conduction method. The cooling curves obtained were superimposed on the continuous cooling transformation (CCT) diagram of AISI 1060 steel, and the resultant microstructure and hardness were estimated.

Experimental

SS probes with diameters of 25 and 50 mm were used to study the effect of section thickness during quenching. The quench probes had a height of 30 mm. A sketch of quench probes with provisions for thermocouples are shown in **Fig. 1**. The thermocouples used

FIG. 1

Sketch of steel probes showing thermocouple locations.

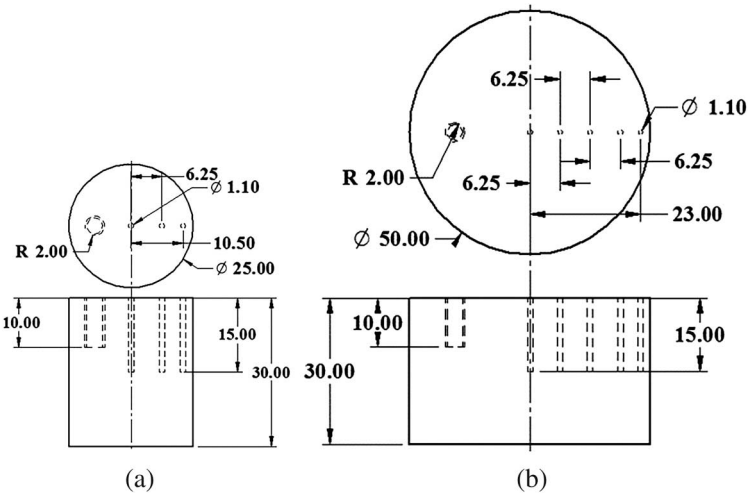

were 1.0 mm in diameter. Holes of 1.1 mm in diameter were drilled to accommodate thermocouples of 1 mm in diameter. The probe was held vertically in the electric furnace using a 304 SS rod that was fastened to the probe at the threaded hole shown as R 2.00 in Fig. 1.

The probes were heated to 860°C and then quenched in the oil quench medium. A pneumatic quench system schematically shown in Fig. 2 consisting of a pneumatic cylinder, a 3/2 solenoid valve, an electric resistance furnace, and a quench tank was used to conduct the quenching experiments. The SS probes with diameters of 25 and 50 mm were

FIG. 2

Schematic of the pneumatic quench system.

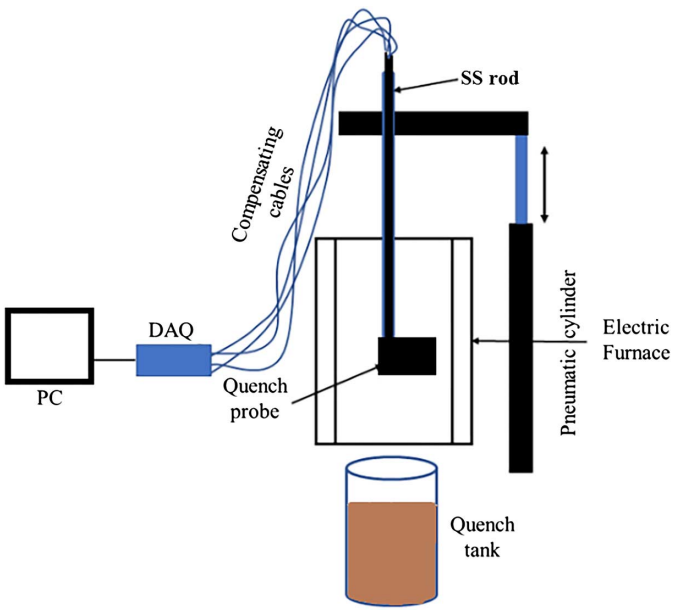

quenched into a tank containing 4 L and 15 L of quench medium, respectively. K- type thermocouples were used to measure the thermal history in the probes during quenching. The embedded thermocouples were connected to a personal computer (PC) via a data acquisition module (NI 9213). The temperature data measured were recorded at an interval of 0.1 s. To minimize end effects during quenching, zirconia, alumina, and sodium silicate insulation paste was used. The top and bottom faces of the probes were coated with this paste. The paste was cured by heating to a temperature of about 180°C. The height of the solidified insulation ranged from 3 to 10 mm. The insulation also served as an entry barrier preventing the quench medium to come into contact with thermocouples. The reduction of heat flow that was due to the application of the paste was checked by coating it over the surface of an inconel probe that was instrumented with a thermocouple. It was found that the application of paste reduced the peak cooling rate by about 96 % during quenching in water.

Interfacial Heat Flux Transients

The spatiotemporal heat flux transients at the metal/quenchant interface were estimated by an inverse heat conduction technique using the near surface thermocouples data. For this purpose, the thermal conductivity, specific heat, and density of the quench probe are given in Table 1. The heat flux was obtained in accordance with the procedure detailed in the work of Kumar [10].

Fig. 3 shows two-dimensional axisymmetric models of the quench probes. These models were used to estimate the boundary heat flux transients (q). The models were meshed uniformly with four node quadrilateral elements. Measured temperature data obtained during the quenching experiment were provided as inputs to these models at nodes corresponding to the locations given in Fig. 1. In the case of the 25-mm steel quench probe, TC, T1, and T2 represent the thermocouples placed at a depth of 15 mm and were positioned at the geometric center, 6.25 mm and 10.5 mm from the center. TC, T1, T2, T3, and

TABLE 1

Thermophysical data for stainless steel probes (JMatPro, Sente Software Ltd., Surrey Research Park, United Kingdom).

Temperature, °C	Thermal Conductivity, W/mK	Specific Heat, J/kgK	Density, kg/m^3
52	21.25	584	7,628.9
152	22.5	648	7,596.29
202	23.1	671.4	7,580.4
252	23.72	738.4	7,563.6
302	24.3	801.4	7,546.4
352	24.87	886	7,528.9
402	25.42	840.8	7,511.17
452	25.97	760.2	7,493.07
502	26.53	721.8	7,474.66
552	27.1	702	7,455.96
602	27.67	691.8	7,436.96
652	28.25	687.4	7,417.6
702	28.84	687.2	7,398.1
752	29.42	689.4	7,378.25
802	30	693.8	7,358.12
852	30.59	699.6	7,337.74

FIG. 3

Axisymmetric meshed model of the steel probes of diameters (a) 25 mm and (b) 50 mm.

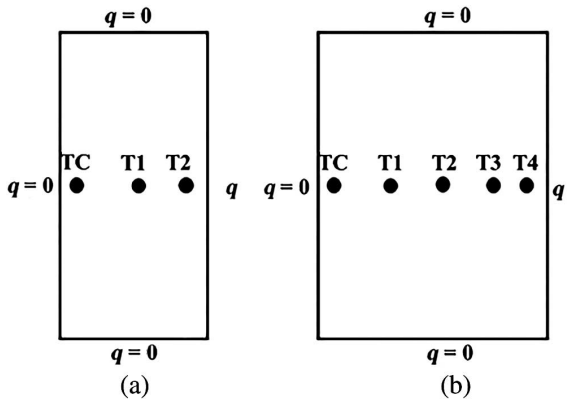

T4 in Fig. 3b represent temperatures obtained at the geometric center 6.25, 12.5, 18.75, and 23 mm from the center and were obtained at a depth of 15 mm. The meshing of the models resulted in 1,500 for the 25-mm section diameter and 3,000 for the 50-mm section size. The convergence limit in the Gauss-Siedel iterations was set as 10^{-6}.

Results and Discussion

The cooling curve and the cooling rate curves obtained during quenching of the 25-mm-diameter probe in oil quenching media are shown in Figs. 4 and 5, respectively. The cooling curves show that, initially, the cooling of the probe by the oil medium was slow because of the insulating nature of the vapor phase stage that surrounded the probe. With continued cooling, the heat required for sustaining the vapor was not enough, which led to its collapse, causing fresh quench medium to contact the probe. This caused an increase in the cooling of the probe accompanied by numerous bubbles that formed and departed from the probe, carrying away larger quantities of heat compared to the heat lost during the vapor phase stage. Thereafter, the heat loss from the probe again reduces as the cooling continues via the convective mode of heat transfer when the temperature of the probe surface drops below the boiling point of the oil, thereby completing the quenching process.

The time of rewetting of the quench medium on the probe surface at the depth of 15 mm was found to be 5.5, 3.8, 3, and 4.6 s during quenching with the 25-mm probe in mineral, sunflower, karanja, and neem oil, respectively. The corresponding values with the 50-mm probe were 5.1, 5.6, 4.6, and 5 s for mineral, sunflower, karanja, and neem oil quenching media, respectively. The peak cooling rate (CR_{max}), temperature (T_{max}), and time (t_{max}) for the 25- and 50-mm probes during quenching in oil media are given in Table 2. The surface temperature data shown in the table are the measured temperature data obtained using a thermocouple positioned at a depth of about 2 mm beneath the surface of the probe. It shows that the cooling rate at the center of the 25-mm section diameter was reduced by over 50 % compared to the maximum cooling rate obtained at its surface during quenching in oils. The largest drop in the maximum cooling rate at the probe center compared to the surface occurred during quenching in mineral oil followed by karanja, neem, and sunflower oil. The temperature at which the maximum cooling rate occurred at the surface was higher with karanja oil followed by neem,

FIG. 4

Cooling curves and cooling rate curves obtained during quenching of the 25-mm probe in (a) mineral, (b) sunflower, (c) karanja, and (d) neem oil quench media.

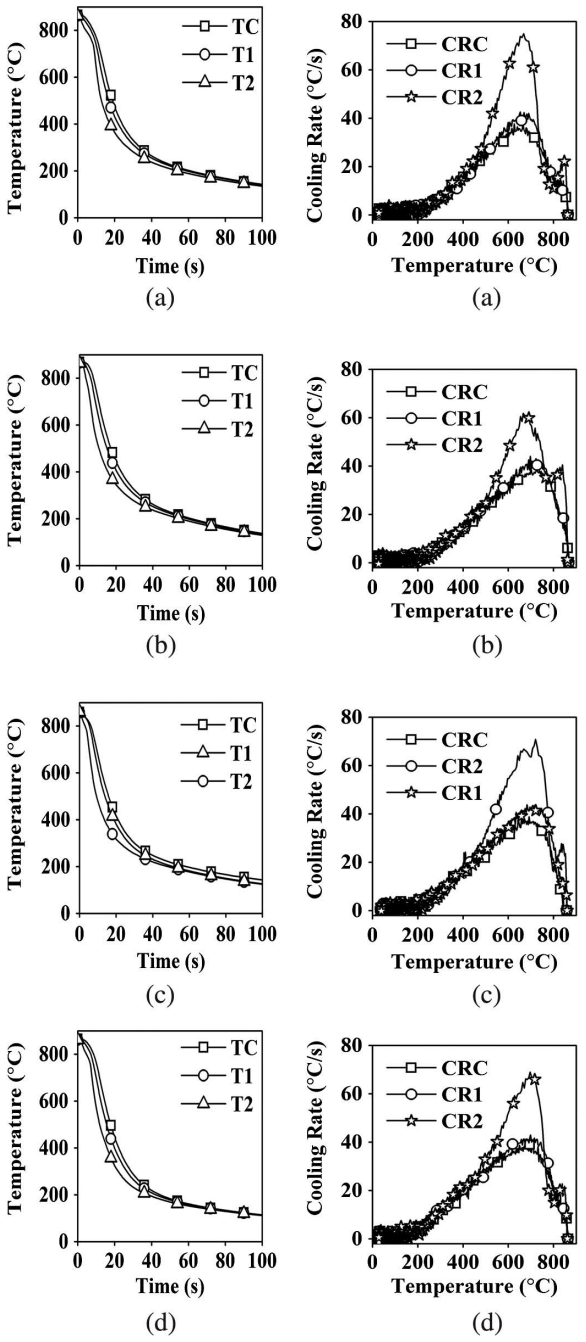

sunflower, and mineral oil. In the case of the 50-mm probe, sunflower oil had the highest cooling rate at the surface, followed by karanja, neem, and mineral oil quenching media. However, at the center of the probe, the maximum cooling rate was the least with sunflower oil followed by karanja oil, and neem and mineral oil had similar peak cooling rates. The peak cooling rate temperature at the surface of the 50-mm probe was the highest with

FIG. 5

Cooling curves and cooling rate curves obtained during quenching of the 50-mm probe in (a) mineral, (b) sunflower, (c) karanja, and (d) neem oil quench media.

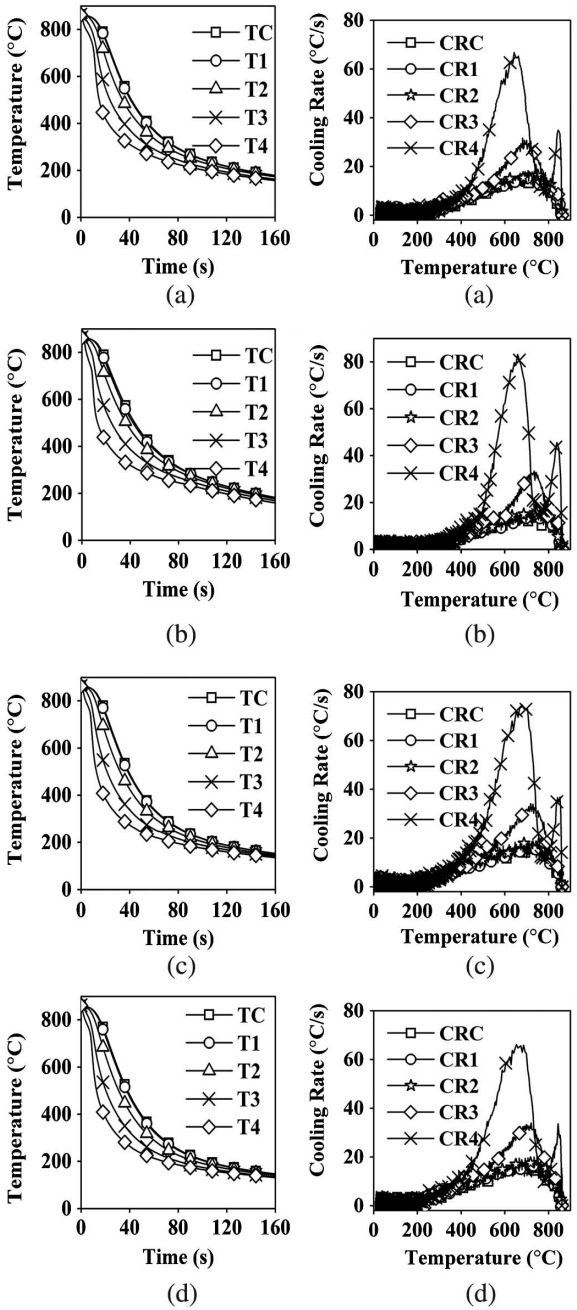

karanja oil, followed by neem, sunflower, and mineral oil, and was similar to the results obtained during quenching of the 25-mm probe.

The peak cooling rates and the temperature obtained during end quenching of a 50-mm-diameter SS test piece were assessed by Prabhu and Fernandes [11]. Their research findings clearly showed that the palm oil used had higher cooling (16°C/s) ability compared to mineral oil (13°C/s). The findings in this study are also in agreement with those

TABLE 2
Peak cooling rate parameters during quenching of 304 SS of section diameters 25 and 50 mm.

	304 Stainless Steel					
	25-mm Section Diameter					
	Center			Surface		
Quenchants	CR_{max}, °C/s	T_{max}, °C	t_{max}, s	CR_{max}, °C/s	T_{max}, °C	t_{max}, s
Mineral oil	37	626	14.6	75	667	9.6
Sunflower oil	39	700	10.4	62	666	6.4
Karanja oil	39	691	9.6	71	720	4.9
Neem oil	39	694	12	69	696	7.8
	50-mm Section Diameter					
Mineral oil	17	682	26	67	643	11.7
Sunflower oil	15	750	21.1	83	659	9.1
Karanja oil	16	666	25.9	74	682	8.6
Neem oil	17	702	22.7	63	679	8.8

published by Agboola et al. [12] who showed increased cooling power with higher hardness during quenching of a medium carbon steel in palm kernel oil (50°C/s) and mineral-vegetable oil blends (between 25°C/s and 42°C/s) compared to mineral oil (28°C/s).

Table 2 also shows that the cooling rate at the center of the 50-mm probe was reduced by over one half of the cooling rate observed at the center of the 25-mm probe during quenching. This clearly indicates that increased section diameter significantly reduced the cooling rate at the center of the probe and increased the time to attain maximum cooling rate at least by a factor of two.

The heat flux transients obtained during quenching of the 25- and 50-mm probes in various quenching oils versus surface temperature estimated are shown in Fig. 6. The nature of the heat flux curve is similar to that of the cooling rate curves. Initially, the heat flux has a low value because of the insulating nature of the vapor phase that surrounded the probe. A maximum occurs during the vapor phase stage called the first critical heat flux. Heat flux then rises rapidly to attain a maximum (second critical heat flux) during the nucleate boiling stage as large quantities of heat are extracted by the quenching medium. The heat flux curves then begin to decrease, and they are lowered as the cooling enters the convective cooling stage.

Because of its larger size, the 50-mm probe's heat flux curves have higher peak flux compared to the 25-mm probe. The peak heat flux was found to be 2.35, 2.27, 2.14, and 2.22 MW/m^2 during quenching of the 25-mm probe in mineral, karanja, sunflower, and neem oils, respectively. The corresponding values for the 50-mm probe were 2.43, 2.67, 2.84, and 2.46 MW/m^2, respectively. Higher peak heat flux was obtained during quenching in oil quench media with a section diameter of 44 mm, which was larger compared to the smaller section diameter of 28 mm [13]. The present results are consistent with this observation and show higher peak flux values for the larger-sectioned SS probe compared to the smaller diameter probe. The ratios of the first critical heat flux to that of the second critical heat flux were 0.32, 0.59, 0.37, and 0.31 during quenching of the 25-mm probe in mineral, sunflower, karanja, and neem oil, respectively. The corresponding values obtained during quenching of the 50-mm probe in mineral, sunflower, karanja, and neem oil were 0.49, 0.54, 0.46, and 0.43, respectively. An intriguing difference between the various oils is clearly indicated in the case of quenching with sunflower oil. Its ratio of first critical to the

FIG. 6

Heat flux transients estimated during quenching of the 25- and 50-mm SS probe in (a) mineral, (b) sunflower, (c) karanja, and (d) neem oil quenching media.

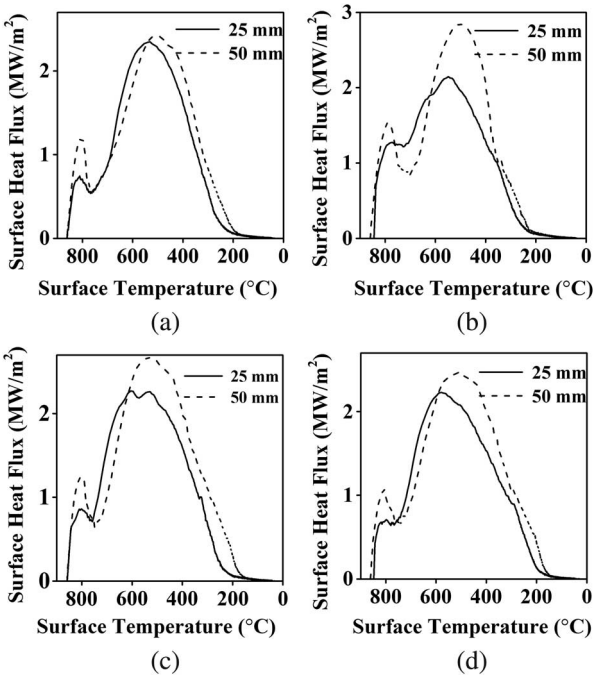

second critical heat flux was higher (0.59). This indicates that larger amounts of heat were removed at slower rates during the vapor phase stage of the sunflower oil quenching medium compared to quenching in other oils. This fact is more clearly evident from the heat-removed curves plotted as a function of the surface temperature in Fig. 7.

The figure also shows the cooling performance of the oil quench media. For the 25-mm probe, heat removed by sunflower oil was lower than the other oils up to a temperature of 700°C. A lower amount of heat was removed by mineral, karanja, and neem compared to sunflower oil between 450°C and 390°C. The amount of heat removed with temperature is higher for mineral, karanja, and sunflower oil compared to neem oils in

FIG. 7

Heat removed versus surface temperature during quenching of (a) 25-mm and (b) 50-mm section diameter probes in various quenching oils.

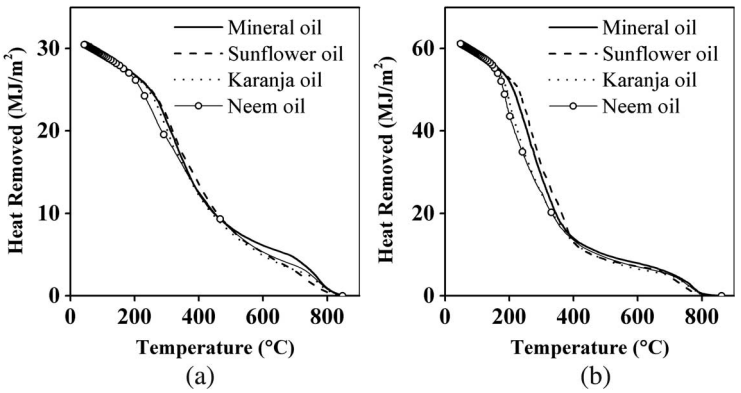

the temperature range of 390°C to 200°C. Lower amounts of heat removed in a certain temperature range implies a faster heat removal rate. For the 50-mm probe, more heat was removed by the mineral and sunflower oil compared to the nonedible quench oils after 400°C.

The quench performance of oils was quantified by superimposing the cooling curves measured at the center and the surface on the CCT diagram of AISI 1060 steel. It should be noted that cooling curve analysis was carried out using an SS probe, which does not undergo phase transformation during quenching. However, superimposition of such cooling curves on the steel CCT diagram can provide meaningful insights about the performance of the quench media. The superimposed cooling curves obtained at the center and near the surface of the 25- and 50-mm probes are shown in Figs. 8 and 9, respectively.

The resultant phase fractions of micro-constituents that are due to quenching are shown in Tables 3 and 4 for 25- and 50-mm probe, respectively. For the 25-mm probe, Table 3 shows that higher martensitic phase fraction is obtained during quenching with

FIG. 8 Measured cooling curves obtained at the (a) center and (b) surface of the 25-mm probe superimposed on the CCT curve of AISI 1060 steel.

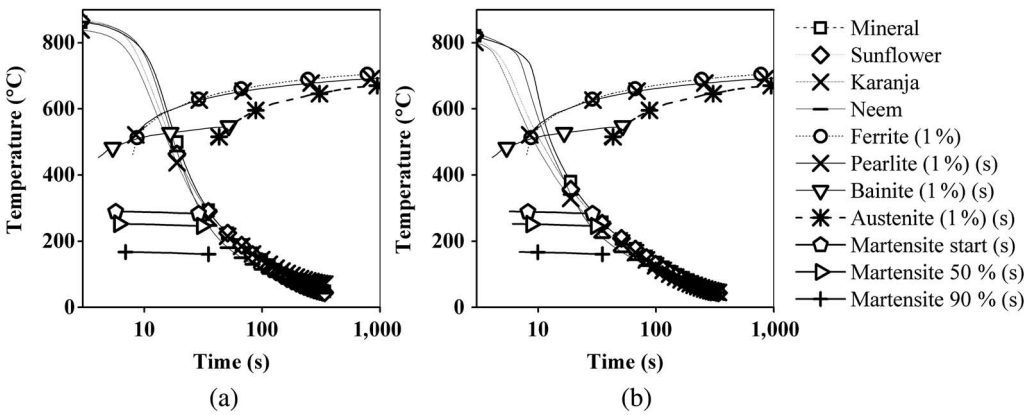

FIG. 9 Measured cooling curves obtained at the (a) center and (b) surface of the 50-mm probe superimposed on the CCT curve of AISI 1060 steel.

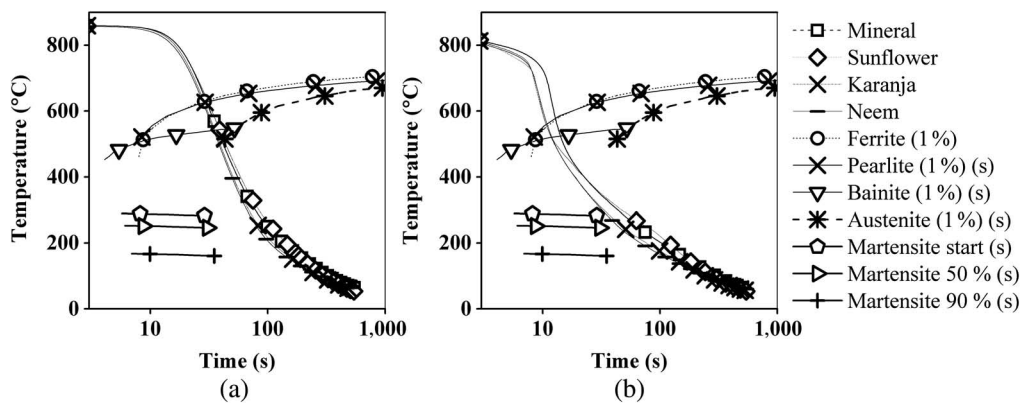

TABLE 3
Phase fractions obtained in 25-mm AISI 1060 steel during quenching in various oils.

Center	Micro constituents	Mineral	Sunflower	Karanja	Neem
	Ferrite fraction, %	2.4	2.2	2.2	2.1
	Pearlite fraction, %	2.5	1.8	2.0	1.3
	Bainite fraction, %	52.4	46.2	47.3	43.6
	Martensite fraction, %	42.4	49.5	48.2	52.5
	Austenite fraction, %	0.3	0.4	0.4	0.4
Surface	Ferrite fraction, %	1.7	1.3	1.1	1.4
	Pearlite fraction, %	1.4	1.0	0.8	1.0
	Bainite fraction, %	33.4	22.9	16.7	24.3
	Martensite fraction, %	63.0	74.2	80.9	72.8
	Austenite fraction, %	0.5	0.5	0.6	0.5

TABLE 4
Phase fractions obtained in 25 mm AISI 1060 steel during quenching in various oils.

Center	Micro Constituents	Mineral	Sunflower	Karanja	Neem
	Ferrite fraction, %	2.7	2.9	2.6	2.5
	Pearlite fraction, %	26.4	33.9	19.6	19.3
	Bainite fraction, %	70.9	63.1	77.9	78.2
	Martensite fraction, %	0.0	0.0	0.0	0.0
	Austenite fraction, %	0.0	0.0	0.0	0.0
Surface	Ferrite fraction, %	2.4	2.1	2.0	2.1
	Pearlite fraction, %	2.6	1.5	0.8	1.5
	Bainite fraction, %	54.1	44.4	40.1	44.5
	Martensite fraction, %	40.6	51.6	56.7	51.4
	Austenite fraction, %	0.3	0.4	0.4	0.4

neem oil followed by sunflower, karanja, and mineral oil, respectively. At the surface, the fraction of martensite is found to be higher with karanja oil, followed by sunflower, neem, and mineral oil. In the case of the 50-mm probe (Table 4), no martensite phase fraction is found at the center of the probe, indicating lower hardness at the center relative to that found at the center of the 25-mm probe. Bainite phase fraction was maximum at the center during quenching with neem oil, followed by karanja and mineral, and sunflower oil had the lowest phase fraction of bainite. At the surface, highest martensite phase fraction was obtained with karanja oil. Sunflower and neem oil quenched steel had similar phase fractions to martensite, and the lowest amount is found with mineral oil quenched steel. The predicted hardness values obtained in the 25-mm probe at its center were 561, 549, 544, and 523 HVN during quenching in neem, sunflower, karanja, and mineral oil, respectively. At the surface, the corresponding values were 625, 630, 650, and 594 HVN. For the 50-mm probe, the hardness values were found to be 323, 323, 316, and 306 HVN with karanja, neem, mineral, and sunflower oil, respectively. The corresponding values at the surface were 579, 557, 516, and 558 HVN, respectively.

Civera et al. [14] measured the hardness during quenching of steel in soybean oil, epoxidized soybean oil (ESO), fatty acid methyl ester soybean oil (FAME), and combinations of ESO-FAME, and compared it with mineral oils. Their results show a hardness (about 638 HVN) obtained in steel that is due to quenching in vegetable oils; this hardness value is higher than that found in mineral oils (620 HVN).

Conclusions

(1) The shortest vapor phase stage duration resulted during quenching with karanja oil.
(2) The larger section diameter probe resulted in a higher peak heat flux relative to that found in the smaller section diameter probe. The peak heat flux was higher in vegetable oils than in mineral oils.
(3) The critical heat flux ratio indicated a higher value during quenching in sunflower oil, implying a larger heat flow during the vapor phase stage relative to the nucleate boiling stage compared to the other oils.
(4) Nonedible vegetable oils of karanja and neem showed faster heat removal compared to mineral oil.
(5) The predicted hardness was found to be higher with karanja oil.

References

[1] Luty, W., "Cooling Media and Their Properties," *Quenching Theory and Technology*, 2nd ed., CRC Press, Boca Raton, FL, 2010, pp. 359–444.
[2] Ramesh, G. and Prabhu, K. N., "Wetting and Cooling Performance of Mineral Oils for Quench Heat Treatment of Steels," *ISIJ Int.*, Vol. 54, No. 6, 2014, pp. 1426–1435, https://doi.org/10.2355/isijinternational.54.1426
[3] Totten, G. E., Bates, C. E., and Clinton, N. A., "Quenching Oils," *Handbook of Quenchants and Quenching Technology*, ASM International, Materials Park, OH, 1993, pp. 129–160.
[4] Totten, G. E., Tensi, H. M., and Lainer, K., "Performance of Vegetable Oils as a Cooling Medium in Comparison to a Standard Mineral Oil," *J. Mater. Eng. Perform.*, Vol. 8, No. 4, 1999, pp. 409–416, https://doi.org/10.1361/105994999770346693
[5] Rose, A., "Das Abkühlungsvermögen von Stahl-Abschreckmitteln," *Arch. für das Eisenhüttenwes*, Vol. 13, No. 8, 1940, pp. 345–354, https://doi.org/10.1002/srin.194000899
[6] de Souza, E. C., Fernandes, M. R., Augustinho, S. C. M., de Campos Franceschini Canale, L., and Totten, G. E., "Comparison of Structure and Quenching Performance of Vegetable Oils," *J. ASTM Int.*, Vol. 6, No. 9, 2009, pp. 1–25, https://doi.org/10.1520/JAI102188
[7] Ramesh, G. and Prabhu, K. N., "Wetting Kinetics, Kinematics and Heat Transfer Characteristics of Pongamia Pinnata Vegetable Oil for Industrial Heat Treatment," *Appl. Therm. Eng.*, Vol. 65, Nos. 1–2, 2014, pp. 433–446, https://doi.org/10.1016/j.applthermaleng.2014.01.011
[8] Adekunle, A. S., Adebiyi, K. A., and Durowoju, M. O., "Impact of Quench Severity and Hardness on AISI 4137 Using Eco-Friendly Quenchants as Industrial Heat Treatment," *J. Mech. Eng. Sci.*, Vol. 4, 2013, pp. 409–417, https://doi.org/10.15282/jmes.4.2013.5.0038
[9] Ademoh, N. A., "Effect of Nigerian Neem Seed Oil as Austempering Quenchant for Locally Recycled Mild Steel," *Middle-East J. Sci. Res.*, Vol. 23, No. 1, 2015, pp. 110–118.
[10] Kumar, T. S., "A Serial Solution for the 2-D Inverse Heat Conduction Problem for Estimating Multiple Heat Flux Components," *Numer. Heat Transfer, Part B*, Vol. 45, No. 6, 2004, pp. 541–563, https://doi.org/10.1080/10407790490277940
[11] Prabhu, K. N. and Fernandes, P., "Effect of Surface Roughness on Metal/Quenchant Interfacial Heat Transfer and Evolution of Microstructure," *Mater. Des.*, Vol. 28, No. 2, 2007, pp. 544–550, https://doi.org/10.1016/j.matdes.2005.08.005
[12] Agboola, J. B., Abubakre, O. K., Mudiare, E., and Adeyemi, M. B., "Performance Assessment of Vegetable Oil and Mineral Oil Blends during Heat Treatment of

Medium Carbon Steel," *Int. J. Microstruct. Mater. Prop.*, Vol. 11, Nos. 3–4, 2016, pp. 203–213, https://doi.org/10.1504/ijmmp.2016.079141

[13] Fernandes, P. and Prabhu, K. N., "Effect of Section Size and Agitation on Heat Transfer during Quenching of AISI 1040 Steel," *J. Mater. Process. Technol.*, Vol. 183, No. 1, 2007, pp. 1–5, https://doi.org/10.1016/j.jmatprotec.2006.08.028

[14] Civera, C., Rivolta, B., Simencio-Otero, R. L., Lúcio, J. G., Totten, G. E., and Canale, L. C. F., "Vegetable Oils as Quenchants for Steels: Residual Stresses and Dimensional Changes," *Mater. Perform. Charact.*, Vol. 3, No. 4, 2014, pp. 306–325, https://doi.org/10.1520/MPC20140039